



Transport properties of ZnTe:N thin films

Hang Chi,¹ Chihyu Chen,² Jamie D. Phillips,² and Ctirad Uher^{1,a)}

¹Department of Physics, University of Michigan, Ann Arbor, Michigan 48109-1040, USA

²Department of Electrical Engineering and Computer Science, University of Michigan, Ann Arbor, Michigan 48109-2122, USA

(Received 8 June 2013; accepted 12 July 2013; published online 25 July 2013)

Highly mismatched alloys have been predicted to exhibit enhanced thermoelectric properties. Here we report on transport properties of one such system, nitrogen-doped ZnTe epitaxial layers on GaAs (100). Hall effect, electrical resistivity, and Seebeck coefficient measurements were performed between 5 K and 300 K for samples with a room temperature hole concentration of $0.34\text{--}2.16 \times 10^{19} \text{ cm}^{-3}$. Significant phonon-drag thermopower reaching $1.5\text{--}2.5 \text{ mV K}^{-1}$ was observed. Fermi-Dirac statistics was used to analyze the transport parameters of ZnTe:N films assuming a single parabolic band. The power factor demonstrates a measurable improvement with increasing nitrogen concentration.

© 2013 AIP Publishing LLC. [<http://dx.doi.org/10.1063/1.4816815>]

ZnTe is a direct wide band gap [2.27 eV at 300 K (Ref. 1)] II-VI semiconductor with zincblende crystal structure, utilized in optoelectronic applications including green light emitting diodes² and solar cells.³ Recently, highly mismatched alloys (HMAs) of II-VI compounds, formed by alloying isovalent constituents with vastly different electronegativities (e.g., ZnSe_{1-x}O_x), have been proposed as candidate materials for promising thermoelectric performance.⁴ The optimistic prediction is based on an assumption that such materials would possess an enhanced power factor defined as $PF = S^2\sigma$, where S is the Seebeck coefficient or thermopower and σ is the electrical conductivity. Practically, however, codoping of additional species is required in order for such isoelectronic HMAs to function with the desired carrier concentration. An alternative approach of forming nonisoelectronic HMAs may provide a solution. Historically, nitrogen has proven to be a controllable p -type dopant in ZnTe (Refs. 5–7) with hole concentrations of up to 10^{20} cm^{-3} . Nevertheless, systematic studies of the thermoelectric properties of such nitrogen doped p -type ZnTe (ZnTe:N) thin films remain largely unknown in the literature. In this letter, a series of ZnTe:N epitaxial layers with varying N content is studied to examine their temperature dependent thermoelectric properties.

ZnTe:N materials were grown on semi-insulating GaAs (100) substrate by molecular beam epitaxy (MBE) using solid source effusion cells for Zn and Te and an electron cyclotron resonance plasma source for nitrogen incorporation. Thickness of the ZnTe:N films (1–2 μm) was determined by analyzing optical reflectance spectral data, whose details were described elsewhere.⁸ Photoluminescence (PL) spectra of the ZnTe:N films were collected at 20 K using excitation from a He-Cd 325 nm laser, a grating spectrometer, lock-in amplification, and a photodiode detector. Rectangular-shaped samples for Hall-effect measurements (2 mm \times 6 mm) and Seebeck coefficient (3 mm \times 10 mm) characterization were cut out of the as-grown sample (10 mm \times 10 mm) by a diamond saw, with the sample glued on an aluminum block

using crystal bond. The residual glue was carefully removed using acetone and then flushed by methanol for 3 min. Tiny indium contacts were soldered on to the sample. Silver epoxy contacts were also used on selected fresh samples in order to double check transport results, which confirmed that none of the phenomena reported in this letter are artifacts possibly induced by indium contacts becoming superconducting at low temperatures. Hall coefficient R_H and electrical resistivity ρ measurements were performed on the same sample from 5 K to 300 K in a Quantum Design Magnetic Property Measurement System (MPMS), equipped with a 5.5 T superconducting magnet, using a Linear Research ac bridge with 16 Hz excitation. Results from warming and cooling cycles were identical. Hall data were taken for both positive and negative magnetic fields to eliminate effects due to probe misalignment. The Hall resistance is linear in terms of the applied magnetic field. The concentration of holes and their Hall mobility were then estimated from the Hall coefficient and the electrical resistivity. For comparison, the amount of incorporated nitrogen atoms in selected samples was characterized using secondary ion mass spectrometry (SIMS). The Seebeck coefficient S and the electrical resistivity ρ were measured from 2 K to 300 K in a home-made cryostat equipped with a radiation shield, using a longitudinal steady-state technique.^{9,10} The base temperature of the sample holder is controlled via a Lakeshore 340 temperature controller. For measurements of the Seebeck coefficient ($S = \Delta V / \Delta T$), one end of the sample was clamped to a copper heat sink, and the other end was provided with a current-driven strain gauge heater as the heat source. Temperature gradients along the length of the sample were monitored using Chromel-Gold/Iron (0.07 at. %) thermocouples soldered onto the samples with tiny indium contacts. Fine copper wires (25 μm in diameter) were used as voltage probes. Typical temperature difference between the hot and cold ends of the sample is 0.3 K above the liquid nitrogen temperature and around 0.1 K at the liquid helium temperature range. Different heater power was supplied at various temperatures yielding consistent Seebeck coefficient readings. The measured Seebeck coefficient S was corrected for the contribution from the Cu wires.¹¹ For measurements of the electrical

^{a)}Author to whom correspondence should be addressed. Electronic mail: cuh@umich.edu.

TABLE I. Typical transport coefficients of various ZnTe:N thin films at 300 K, including nitrogen concentration $[N]$ from SIMS measurement, Hall coefficient R_H , hole concentration p , electrical resistivity ρ , Seebeck coefficient S , thermoelectric power factor PF , Hall mobility μ_H , and effective mass m^* .

ID	$[N]$ (10^{19} cm^{-3})	R_H ($\text{cm}^3 \text{ C}^{-1}$)	p (10^{19} cm^{-3})	ρ ($\mu\Omega \text{ m}$)	S ($\mu\text{V K}^{-1}$)	PF ($\mu\text{W m}^{-1} \text{ K}^{-2}$)	μ_H ($\text{cm}^2 \text{ V}^{-1} \text{ s}^{-1}$)	m^* (m_e)
1	...	1.836	0.34	297	380	486	61.8	1.31
2	1.41	1.019	0.61	280	338	408	36.4	1.39
3	...	0.470	1.33	233	297	379	20.2	1.68
4	...	0.398	1.57	157	259	427	25.4	1.38
5	4.14	0.289	2.16	107	232	503	27.0	1.37

resistivity ρ , a current was passed along the length of each sample, and the corresponding voltage was collected via a standard four-probe-technique using Keithley nanovoltmeters. Typical dc current of $10 \mu\text{A}$ was used for the measurement, in order to avoid overheating the sample. Different currents at various temperatures were tried confirming the ohmic nature of contacts and leading to consistent electrical resistivity values. The electrical resistivity measurements using both ac and dc techniques agree with each other. The uncertainties of electrical resistivity, Seebeck coefficient, and Hall coefficient are estimated to be $\pm 3\%$, $\pm 3\%$, and $\pm 5\%$, respectively. Resistance of the substrate at room temperature was larger than $500 \text{ M}\Omega$ and, of course, much larger at low temperatures where interesting transport phenomena were observed. Thus, the electrical signal was solely due to the conducting film.

Typical transport properties of five as-grown ZnTe:N films at 300 K are summarized in Table I. These ZnTe:N films with similar thickness ($1\text{--}2 \mu\text{m}$) demonstrate hole concentrations that range over approximately an order of magnitude ($0.34\text{--}2.16 \times 10^{19} \text{ cm}^{-3}$ at 300 K). While even larger ranges of carrier concentration would be desirable to study, difficulties in controlling nitrogen concentration at lower levels, as well as measuring parameters for lower nitrogen concentration (particularly at low temperature where resistivity is high), prohibited inclusion in this study. We have labeled samples in the order of increasing hole concentration at 300 K to facilitate the following discussion.

Temperature dependent Hall measurements of all samples show unanimously positive Hall coefficient R_H at all temperatures, implying the p -type conduction of ZnTe:N. The estimated hole concentration p [$=1/(e \cdot R_H)$, where e is the elementary charge] for all samples from 5 K to 300 K is plotted in Fig. 1(a). The increasing hole concentration from sample 1 to sample 5 is a direct result of increasing nitrogen incorporation, as suggested by the SIMS measurements of nitrogen concentration $[N]$ in the films (SIMS tests were limited to only two samples due to the experimental cost and schedule). Approximately, a factor of two larger nitrogen concentration is measured by SIMS in comparison to the hole concentration measured by the Hall effect. The apparent doping efficiency of nitrogen in these ZnTe:N samples is therefore estimated to be approximately 50%. The Hall mobility μ_H [$=R_H/\rho$ (see Fig. 1(b)) with ρ shown in Fig. 2(a)] of these samples are found to be $20\text{--}60 \text{ cm}^2 \text{ V}^{-1} \text{ s}^{-1}$ at room temperature, in agreement with literature values^{7,12} for samples with a similar doping level.

As shown in Fig. 2(a), the increasing amount of nitrogen incorporation (from samples 1–5) improves the overall

electrical conductivity due to higher carrier concentration and also exhibits a surprising qualitative change in the temperature dependence of electrical resistivity. At the highest doping levels (samples 4 and 5, $p > 1.5 \times 10^{19} \text{ cm}^{-3}$), the electrical resistivity has a positive temperature coefficient over most of the temperature range, i.e., electrical resistivity increases as temperature increases. This is a typical behavior of the heavily doped degenerate semiconductor. Note that acceptor formation via nitrogen incorporation in ZnTe is typically attributed to the substitution of N on the lattice sites of Te, resulting in an acceptor activation energy of 46 meV.¹² At such high doping levels, acceptor states originated from nitrogen impurity likely form an impurity band, as implied by the nearly temperature independent hole concentration in Fig. 1(a). As the nitrogen incorporation is gradually reduced from this highly doped regime (samples 3, 2, and 1), the electrical resistivity profile deviates from a simple metallic behavior, with a peak observed in the temperature range between 50 K and 100 K. This could be related to the more subtle details of the nitrogen induced impurity level/band in ZnTe, which requires further investigation. To shed more light on the effect of N-doping, PL spectra of various ZnTe:N samples, together with a pure ZnTe sample as

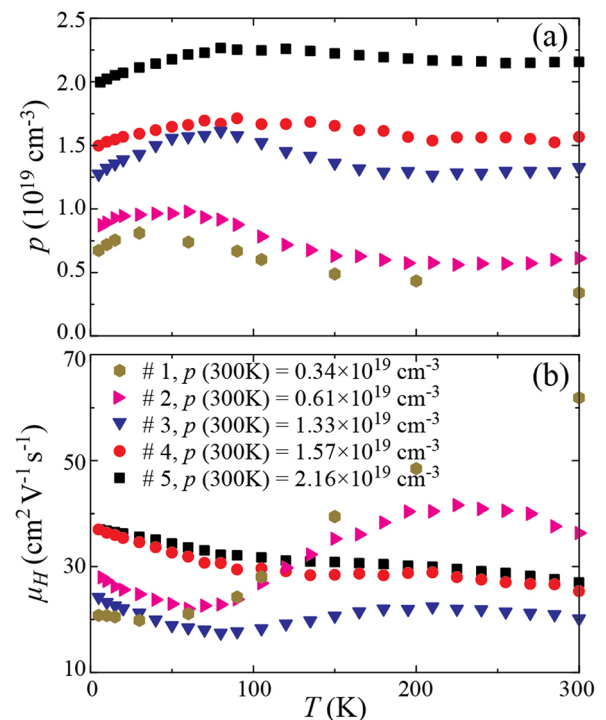


FIG. 1. Temperature dependent (a) hole concentration p (b) Hall mobility μ_H of ZnTe:N MBE thin films with various doping levels.

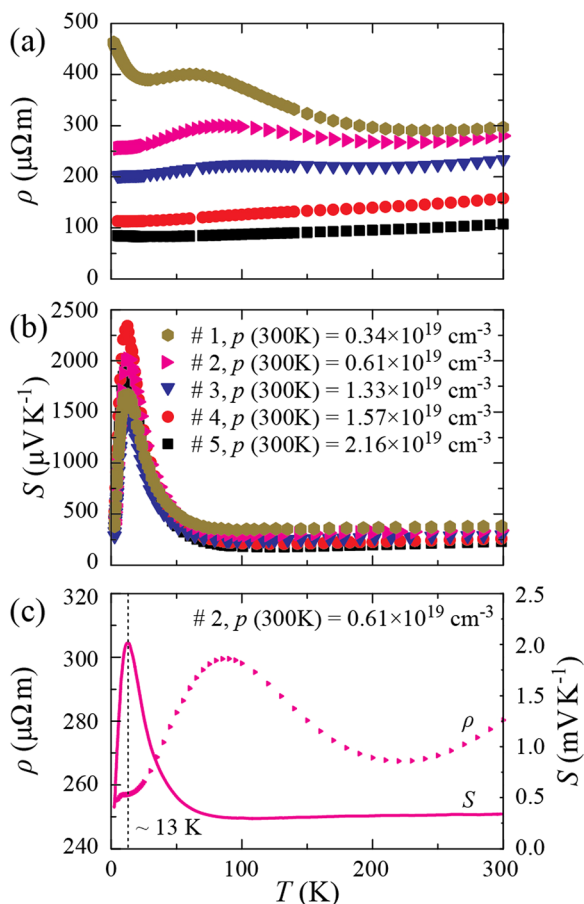


FIG. 2. Temperature dependent (a) electrical resistivity ρ and (b) Seebeck coefficient S of ZnTe:N MBE thin films with various doping levels. (c) A correlation between the Seebeck coefficient peak (~ 13 K) and an electrical resistivity plateau in sample 2, suggesting that phonon drag leaves an imprint on the temperature profile of the electrical resistivity.

reference, were collected at 20 K. They reveal a red shift of the band edge peak upon N-doping, as shown in Fig. 3. This effect may correspond to the formation and broadening of the nitrogen induced impurity band, as more nitrogen atoms are incorporated into the system.

Figure 2(b) shows a plot of the temperature dependent Seebeck coefficient S of the ZnTe:N films. S is positive for all samples suggesting p -type conduction, in agreement with

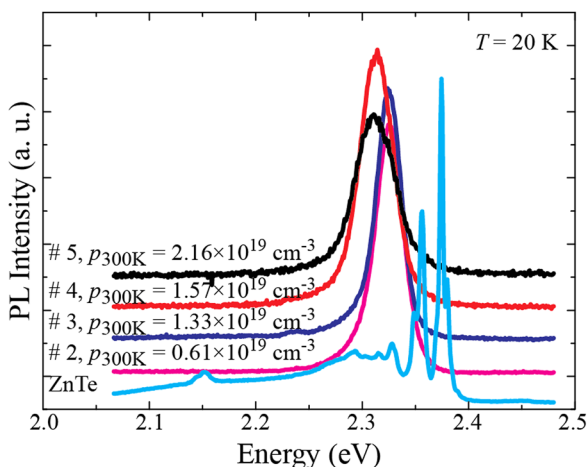


FIG. 3. PL spectra at 20 K of pure ZnTe and ZnTe:N MBE thin films with various doping levels.

the Hall effect measurements. The Seebeck coefficient at 300 K decreases as the concentration of holes increases, which agrees with the typical behavior of a degenerate semiconductor. At the lowest temperatures, S increases rapidly to a maximum at ~ 13 K and then decreases until ~ 100 K.

The greatly enhanced Seebeck coefficient at low temperatures (as high as 1.5 – 2.5 mV K^{-1}) is a manifestation of strong electron-phonon interaction otherwise known as the phonon-drag effect.¹³ The peak position of the phonon-drag Seebeck coefficient (~ 13 K) in ZnTe:N coincides with the peak position of the phonon thermal conductivity in bulk crystals of ZnTe.^{14,15} This is in accord with the concept of the phonon-drag effect. In the presence of a thermal gradient, non-equilibrium phonons impart their momentum to electrons, resulting in a momentary electric current just as an applied electric field would do. However, under an open circuit condition (the condition under which the Seebeck coefficient is measured), an electric field is set up which counters such impulsively generated flow of electrons. By the phonon-drag Seebeck coefficient, one understands the ratio of this induced electric field to the applied thermal gradient. Unlike the diffusion component of the Seebeck coefficient that is present at all temperatures, the phonon-drag contribution is manifested only at temperatures where phonon-electron processes dominate over all other modes of phonon scattering. Practically, this implies low enough temperatures where phonon-phonon Umklapp processes are infrequent, but temperatures not so low that the population of phonons would be very small. Since these same phonons are responsible for heat conduction, the positions of the phonon-drag peak and the peak in the lattice thermal conductivity essentially coincide. It is worthwhile to note that the thermal conductivity of GaAs substrate peaks at a similar temperature of ~ 10 K.^{10,16,17} Thus, any phonons leaking¹⁸ from the substrate into the film might, in principle, also contribute to phonon drag in ZnTe:N grown on GaAs. However, as pointed by Wang *et al.*,¹⁹ for such leaking phonons to make an appreciable contribution to the phonon drag, the film must be very thin (a few tens of nm), and having a near perfect lattice match with the substrate, a situation is difficult to realize in II-VI compounds.

While examples of significant phonon-drag Seebeck effect are often seen in both metals and semiconductors,^{20–22} it is exceptionally rare to see any signature of phonons dragging charge carriers in the electrical resistivity. The reason why phonon-drag effects are easily detected in the Seebeck coefficient and not in the electrical resistivity lies in the fact that the phonon-drag Seebeck effect is a first-order effect in the interaction between non-equilibrium phonons and electrons while it is a second-order effect as far as the electrical resistivity is concerned. Electrons, accelerated by the applied electric field, lose some of their momentum by being scattered by phonons and thus causing a flow of phonons which then acts back on the electrons.²³ We would like to point out that in Fig. 2(c), at the lowest temperatures ~ 13 K, there is a local plateau in the electrical resistivity profile which coincides with the position of the phonon-drag Seebeck effect peak. Upon cooling down, instead of decreasing monotonically, the electrical resistivity tends to (quasi-) saturate in the regime where significant phonon-drag Seebeck effect is

manifested. This result actually might be one of very rare examples where phonon drag exerts an influence in the electrical resistivity. Further experimental and theoretical work is needed to ascertain this point.

At $T > 150$ K, S increases linearly with T , as shown in Fig. 4(a), due to carrier diffusion driven by the temperature gradient. For a p -type degenerate semiconductor, S can be expressed as follows:²⁴

$$S = \frac{k_B}{e} \left[\frac{r + 5/2 F_{r+3/2}(\eta)}{r + 3/2 F_{r+1/2}(\eta)} - \eta \right], \quad (1)$$

where k_B is the Boltzmann constant, e the elementary charge, r the index of energy dependent relaxation time $\tau = \tau_0 \varepsilon^r$ (taken to be $-1/2$ for acoustic phonon scattering), $\eta = E_F/k_B T$ the reduced Fermi level measured from the top the valence band, and $F_j(\eta)$ the j -th Fermi integral given by

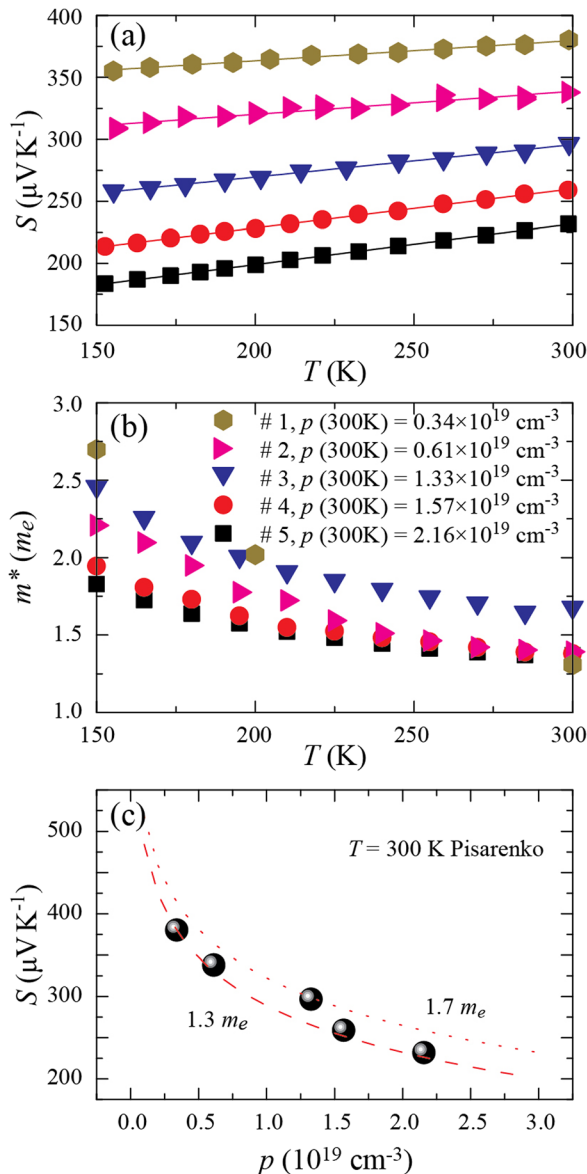


FIG. 4. (a) Seebeck coefficient S and (b) effective mass m^* of ZnTe:N from 150 K to 300 K. (c) Pisarenko plot at 300 K indicating S vs. p relation follows the single parabolic band model.

$$F_j(\eta) = \int_0^\infty \frac{\xi^j}{\exp(\xi - \eta) + 1} d\xi. \quad (2)$$

The carrier concentration is described by Fermi-Dirac statistics according to

$$p = 4\pi \left(\frac{2m^* k_B T}{h^2} \right)^{3/2} F_{1/2}(\eta), \quad (3)$$

where h is the Planck constant and m^* is the effective mass of holes in the valence band. Combining Eqs. (1) and (3), the effective mass can be estimated from the measured S and p data. The temperature dependent m^* is plotted in Fig. 4(b). The observed effective mass (1.3–1.7 m_0 at 300 K) is significantly larger than the effective mass for intrinsic ZnTe ($m_i^* = 0.2 m_0$). This observation is consistent with a modified band structure due to the formation of an impurity band via heavy nitrogen doping. The Pisarenko plot of the Seebeck coefficient versus hole concentration at 300 K is illustrated in the Fig. 4(c), where dashed lines are analytical results from Eqs. (1) and (3) with the effective mass as a fitting parameter. It verifies the validity of the single parabolic band model for the N-doped ZnTe:N system. In addition, with the N-doping level increased, the power factor (PF) improves to $503 \mu\text{W m}^{-1} \text{K}^{-2}$ (see Table I) for the highest doping level explored in this study.

We have performed low temperature thermoelectric characterization on a series of nitrogen doped ZnTe thin films grown by MBE. We have observed a significant phonon-drag peak in the Seebeck coefficient at ~ 13 K in all ZnTe:N samples corresponding to a few mV K^{-1} . Upon tuning the N-doping level, qualitative changes in the temperature dependent electrical resistivity profile develop, leading to a marginal improvement of the power factor at the highest doping level. A single parabolic band model proves to be a valid description for the ZnTe:N system at the doping levels we have explored.

This work was supported by the Center for Solar and Thermal Energy Conversion, an Energy Frontier Research Center funded by the U.S. Department of Energy, Office of Science, Office of Basic Energy Sciences under Award No. DE-SC0000957.

¹S. Adachi, *Properties of Group-IV, III-V and II-VI Semiconductors* (John Wiley & Sons, West Sussex, UK, 2005).

²K. Sato, M. Hanafusa, A. Noda, A. Arakawa, M. Uchida, T. Asahi, and O. Oda, *J. Cryst. Growth* **214/215**, 1080 (2000).

³W. Wang, A. S. Lin, and J. D. Phillips, *Appl. Phys. Lett.* **95**, 011103 (2009).

⁴J.-H. Lee, J. Wu, and J. C. Grossman, *Phys. Rev. Lett.* **104**, 016602 (2010).

⁵J. Han, T. S. Stavrinides, M. Kobayashi, R. L. Gunshor, M. M. Hagerott, and A. V. Nurmikko, *Appl. Phys. Lett.* **62**, 840 (1993).

⁶I. W. Tao, M. Jurkovic, and W. I. Wang, *Appl. Phys. Lett.* **64**, 1848 (1994).

⁷T. Baron, K. Saminadayar, and N. Magnea, *J. Appl. Phys.* **83**, 1354 (1998).

⁸W. Wang, W. Bowen, S. Spanninga, S. Lin, and J. Phillips, *J. Electron. Mater.* **38**, 119 (2009).

⁹J. Yang, G. P. Meisner, D. T. Morelli, and C. Uher, *Phys. Rev. B* **63**, 014410 (2000).

- ¹⁰T. Dannecker, Y. Jin, H. Cheng, C. F. Gorman, J. Buckeridge, C. Uher, S. Fahy, C. Kurdak, and R. S. Goldman, *Phys. Rev. B* **82**, 125203 (2010).
- ¹¹C. Uher, *J. Appl. Phys.* **62**, 4636 (1987).
- ¹²Y. Fan, J. Han, L. He, J. Saraie, R. L. Gunshor, M. Hagerott, and A. V. Nurmikko, *J. Electron. Mater.* **23**, 245 (1994).
- ¹³C. Herring, *Phys. Rev.* **96**, 1163 (1954).
- ¹⁴G. A. Slack, *Phys. Rev. B* **6**, 3791 (1972).
- ¹⁵A. Noguera and S. M. Wasim, *Solid State Commun.* **50**, 483 (1984).
- ¹⁶A. I. Ivanov, A. N. Luk'yanov, B. A. Merisov, A. V. Sologubenko, and G. Y. Khadjai, *Low Temp. Phys.* **28**, 462 (2002).
- ¹⁷M. V. Warren, A. W. Wood, J. C. Canniff, F. Naab, C. Uher, and R. S. Goldman, *Appl. Phys. Lett.* **100**, 102101 (2012).
- ¹⁸M. A. Zudov, I. V. Ponomarev, A. L. Efros, R. R. Du, J. A. Simmons, and J. L. Reno, *Phys. Rev. Lett.* **86**, 3614 (2001).
- ¹⁹G. Wang, L. Endicott, H. Chi, P. Lošfák, and C. Uher, "Tuning the Temperature Domain of Phonon Drag in Thin Films by the Choice of Substrate," *Phys. Rev. Lett.* (in press).
- ²⁰R. Fletcher, V. M. Pudalov, Y. Feng, M. Tsaousidou, and P. N. Butcher, *Phys. Rev. B* **56**, 12422 (1997).
- ²¹R. Fletcher, M. D'Iorio, A. S. Sachrajda, R. Stoner, C. T. Foxon, and J. J. Harris, *Phys. Rev. B* **37**, 3137 (1988).
- ²²R. Fletcher, J. J. Harris, C. T. Foxon, M. Tsaousidou, and P. N. Butcher, *Phys. Rev. B* **50**, 14991 (1994).
- ²³R. P. Huebener, *Phys. Rev.* **146**, 502 (1966).
- ²⁴H. J. Goldsmid, *Electronic Refrigeration* (Pion, London, 1986).